Contents lists available at ScienceDirect

International Communications in Heat and Mass Transfer

Turbulence modeling in a parallel flow moving porous bed ☆

Ana C. Pivem, Marcelo J.S. de Lemos *

Departamento de Energia — IEME, Instituto Tecnológico de Aeronáutica — ITA, 12228-900 São José dos Campos, SP, Brazil

ARTICLE INFO

ABSTRACT

This paper deals with numerical simulation of turbulence in a parallel flow moving bed, in which turbulence is considered in the void spaces occupied by the fluid phase. Volume averaging techniques are applied to both time-mean and statistical flow fields. The set of resulting governing equations is discretized via the control-volume method and the resulting algebraic equation set is solved via the SIMPLE method. Results indicate that for lower values of slip ratio, Darcy number and bed porosity, higher levels of turbulence kinetic energy are computed.

© 2013 Elsevier Ltd. All rights reserved.

1. Introduction

Many applications in industry are concerned with turbulent flow through permeable beds. Examples are found in devices such as gasifiers, in chemical separation equipment and in recuperation of petrochemical processes, to mention a few applications. Within this context, Yang [1] showed numerical simulation of turbulent fluid flow and heat transfer characteristics in heat exchangers fitted with a porous medium, where the permeable material was inserted in a heat exchanger to improve its process performance. Ref. [1] applied the k–ε model to handle turbulence. Further, among many studies reporting results on turbulent gas–solid transport, one can mention the one by Littman et al. [2], who showed the effect of particle diameter, particle density and loading ratio on the drag coefficient in steady turbulent gas–solid transport, Mansoori et al. [3], who presented a thermo-mechanical modeling for turbulence heat transfer in gas–solid flows including particle collisions and Zhang and Reese [4], who studied particle–gas turbulence interactions using a kinetic theory approach applied to granular flows.

Recently, a macroscopic model for turbulence in porous media was proposed and applied to a number of flows including thermal equilibrium [5] as well as non-equilibrium [6] between temperatures of the fixed solid and fluid phases. For cases when the solid phase also moves, computations for turbulent flow were also presented in de Lemos and Saito [7], but therein their study was limited to the investigation of the effect of the relative velocity on the statistical field. In addition, laminar flow and heat transfer studies in a moving porous bed in parallel [8] and in counter flow [9] configurations were also published. In [8,9], a broader study presented the effects of Reynolds number, slip ratio,

porosity and permeability of the medium on heat transfer, but only laminar flow was therein investigated.

Therefore, the purpose of this contribution is to extend the work of [7] on turbulent moving beds, including now a variety of effects shown previously only for laminar flows [8,9], namely the effect of Reynolds number, slip ratio, porosity and permeability of the medium. Here, the focus is on the impact on the levels of turbulent kinetic energy when several flows and medium properties are varied. Further, two turbulence models are here employed, namely the High and Low Reynolds number formulations.

2. Macroscopic model for flow equations

The equations to follow are available in the open literature and for that their derivation is not repeated here [6]. The geometry considered in this work is schematically shown in Fig. 1a. A moving porous bed co-flows with a permeating fluid and both, the solid matrix as well as the working fluid, move in the same west-to-east direction. The channel shown in the figure has length and height given by L and H, respectively. For the sake of completeness, equations for both fixed and moving medium are presented below.

2.1. Fixed bed

A macroscopic form of the governing equations is obtained by taking the volumetric average of the entire equation set. In this development, the porous medium is considered to be rigid, fixed and saturated by the incompressible fluid. The final forms of the equations considered here are given by [6]:

Continuity:

$$\nabla \cdot \overline{\mathbf{u}}_D = 0 \tag{1}$$

Nomenclature

A_i	Interfacial area [m^2]
a_i	Interfacial area per unit volume, $a_i = A_i/\Delta V$ [m^{-1}]
c_F	Forchheimer coefficient
c_K	Non-dimensional turbulence model constant
c's	Model constants
D	Particle diameter [m]
$\mathbf{D}$	Deformation rate tensor, $\mathbf{D} = [\nabla\mathbf{u} + (\nabla\mathbf{u})^T]/2$ [s^{-1}]
f_2	Damping function
f_μ	Damping function
G^i	Production rate of $\langle k \rangle^i$ due to the porous matrix
H	Distance between channel walls [m]
k	Turbulent kinetic energy per unit mass [m^2/s^2]
$\langle k \rangle^i$	Intrinsic (fluid) average of k
$\langle k \rangle^v$	Volume (fluid + solid) average of k
K	Permeability [m^2]
L	Channel length [m]
p	Thermodynamic pressure [N/m^2]
$\langle p \rangle^i$	Intrinsic (fluid) average of pressure p [N/m^2]
Re	Reynolds number based on $\overline{\mathbf{u}}_D$
Re_D	Reynolds number based on $\overline{\mathbf{u}}_{rel}$
$\overline{\mathbf{u}}$	Microscopic time-averaged velocity vector [m/s]
$\langle \overline{\mathbf{u}} \rangle^i$	Intrinsic (fluid) average of $\overline{\mathbf{u}}$ [m/s]
$\overline{\mathbf{u}}_D$	Darcy velocity vector, $\overline{\mathbf{u}}_D = \phi\langle\overline{\mathbf{u}}\rangle^i$ [m/s]
$\overline{\mathbf{u}}_{rel}$	Relative velocity based on total volume, $\overline{\mathbf{u}}_{rel} = \overline{\mathbf{u}}_D - \mathbf{u}_s$ [m/s]
u_τ	Velocity shear stress [m/s]
X	Dimensionless coordinate
y^+	Dimensionless distance between the wall and first grid node, $y^+ = \frac{y_w u_\tau}{\nu}$

Greek

ε	Dissipation rate of k, $\varepsilon = \mu\overline{\nabla\mathbf{u}' : (\nabla\mathbf{u}')^T}/\rho$ [m^2/s^3]
$\langle \varepsilon \rangle^i$	Intrinsic (fluid) average of ε
ϕ	Porosity
γ	Phase identifier
μ	Fluid dynamic viscosity [kg/(m s)]
μ_t	Turbulent viscosity [kg/(m s)]
μ_{t_ϕ}	Macroscopic turbulent viscosity [kg/(m s)]
ν	Kinematic viscosity [m^2/s]
ρ	Density [kg/m^3]
$\sigma_k, \sigma_\varepsilon$	Non-dimensional constants

Subscript

s, f	$s =$ solid, $f =$ fluid

Momentum:

$$\rho\left[\nabla \cdot \left(\frac{\overline{\mathbf{u}}_D \overline{\mathbf{u}}_D}{\phi}\right)\right] = -\nabla\left(\phi\langle\overline{p}\rangle^i\right) + \mu\nabla^2\overline{\mathbf{u}}_D + \nabla \cdot \left(-\rho\phi\langle\overline{\mathbf{u}'\mathbf{u}'}\rangle^i\right) \quad (2)$$

$$-\left[\frac{\frac{\mu\phi}{K}\overline{\mathbf{u}}_D + c_F\phi\rho|\overline{\mathbf{u}}_D|\overline{\mathbf{u}}_D}{\sqrt{K}}\right],$$

Turbulent kinetic energy:

$$\rho\nabla \cdot \left(\overline{\mathbf{u}}_D\langle k \rangle^i\right) = \nabla \cdot \left[\left(\mu + \frac{\mu_{t_\phi}}{\sigma_k}\right)\nabla\left(\phi\langle k \rangle^i\right)\right] + P^i + G^i - \rho\phi\langle\varepsilon\rangle^i \quad (3)$$

Dissipation rate of turbulence kinetic energy:

$$\rho\nabla.\left(\overline{\mathbf{u}}_D\langle\varepsilon\rangle^i\right) = \nabla \cdot \left[\left(\mu + \frac{\mu_{t_\phi}}{\sigma_\varepsilon}\right)\nabla\left(\phi\langle\varepsilon\rangle^i\right)\right] + c_1 P^i\frac{\langle\varepsilon\rangle^i}{\langle k \rangle^i}$$

$$+ c_2\frac{\langle\varepsilon\rangle^i}{\langle k \rangle^i}\left(G^i - \rho\phi\langle\varepsilon\rangle^i\right) \quad (4)$$

where $\overline{\mathbf{u}}_D$ is the Darcy velocity vector, $\overline{\mathbf{u}}_D = \phi\langle\overline{\mathbf{u}}\rangle^i$, ϕ is the porosity, ρ is the density of the fluid, p is the pressure, μ is the fluid dynamic viscosity, K is the medium permeability, c_F is the Forchheimer coefficient, μ_{t_ϕ} is the macroscopic turbulent viscosity, σ_k and σ_ε are constants, $\langle k \rangle^i$ is the intrinsic (fluid) average of k and $\langle\varepsilon\rangle^i$ is the intrinsic dissipation rate of $\langle k \rangle^i$, $\varepsilon = \mu\overline{\nabla\mathbf{u}' : (\nabla\mathbf{u}')^T}/\rho$. In Eq. (4), c_1 and c_2 are constants, $P^i = -\rho\langle\overline{\mathbf{u}'\mathbf{u}'}\rangle^i : \nabla\overline{\mathbf{u}}_D$ is the production rate of $\langle k \rangle^i$ due to gradients of $\overline{\mathbf{u}}_D$ and $G^i = c_k\rho\phi\langle k \rangle^i|\overline{\mathbf{u}}_D|/\sqrt{K}$ is the generation rate of the intrinsic average of k due to the action of the porous matrix (see [6] for details).

2.2. Moving bed

For a moving bed, only cases where the solid phase velocity is kept constant will be considered here, or say, we assume a moving bed with constant velocity that crosses a fixed control volume in addition to a co-flowing fluid. The steps below show first some basic definitions prior to presenting a proposal for a set of transport equations for analyzing moving systems.

A general form for a volume-average of any property φ, distributed within a phase γ that occupies volume ΔV_γ can be written as (Gray and Lee [10], Whitaker [11,12]),

$$\langle\varphi\rangle^\gamma = \frac{1}{\Delta V_\gamma}\int_{\Delta V_\gamma}\varphi dV_\gamma. \quad (5)$$

In the general case, the volume ratio occupied by phase γ will be $\phi^\gamma = \Delta V_\gamma/\Delta V$ where ΔV is the volume of the so-called "Representative Elementary Volume", REV. If there are two phases, a solid $\gamma = s$ and a fluid phase $\gamma = f$, volume average can be established on both regions. Also,

$$\phi^s = \Delta V_s/\Delta V = 1 - \Delta V_f/\Delta V = 1 - \phi^f \quad (6)$$

and for simplicity of notation one can drop the superscript "f" to get

$$\phi^s = 1 - \phi. \quad (7)$$

As such, calling the instantaneous local velocities for the solid and fluid phases, $\mathbf{u}_s$ and $\mathbf{u}$, respectively, one can obtain the average for the solid velocity, within the solid phase, as follows,

$$\langle\mathbf{u}\rangle^s = \frac{1}{\Delta V_s}\int_{\Delta V_s}\mathbf{u}_s dV_s \quad (8)$$

with, in turn, can be related to an average velocity referent to the entire REV as,

$$\mathbf{u}_s = \overbrace{\frac{\Delta V_s}{\Delta V}}^{(1-\phi)}\underbrace{\frac{1}{\Delta V_s}\int_{\Delta V_s}\mathbf{u}_s dV_s}_{\langle\mathbf{u}\rangle^s}. \quad (9)$$

A further approximation herein is that the porous bed is rigid and moves with a steady average velocity $\mathbf{u}_s$. Note that the condition of
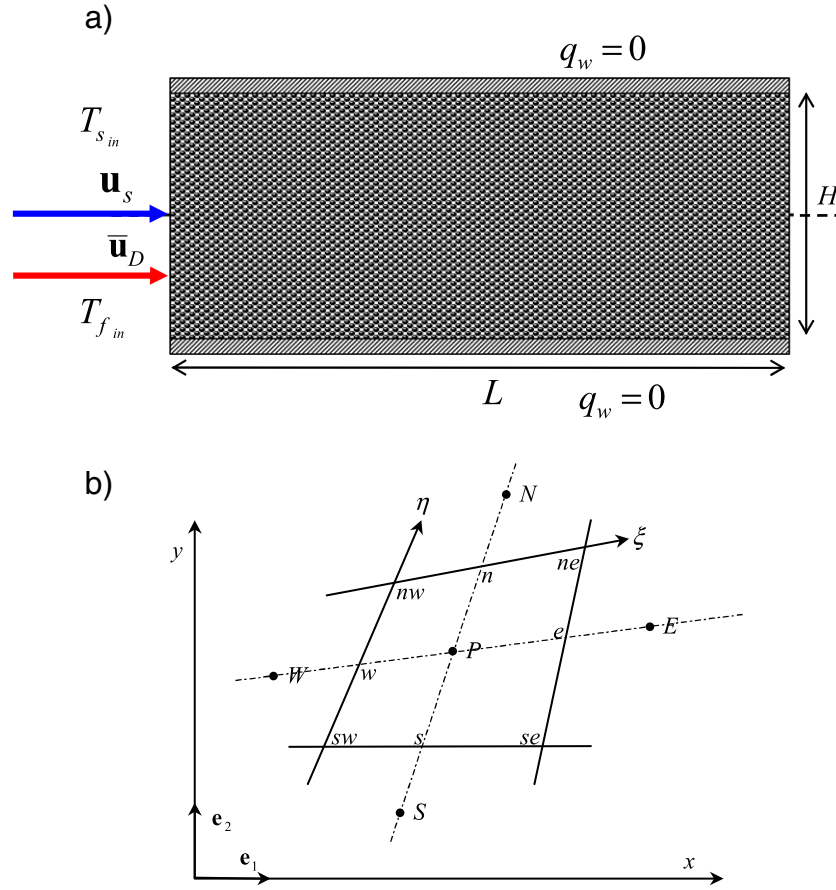
Fig. 1. a) Porous bed reactor with a moving solid matrix; and b) control volume notation.

steadiness for the solid phase gives $\mathbf{u}_s = \overline{\mathbf{u}}_s = const$ where the overbar denotes, as usual in the literature, time-averaging.

For the fluid phase, the intrinsic (fluid) volume average gives, after using the subscript "i" also for consistency with the literature,

$$\langle \overline{\mathbf{u}} \rangle^i = \frac{1}{\Delta V_f} \int_{\Delta V_f} \overline{\mathbf{u}} \, dV_f. \tag{10}$$

Both velocities can then be written as,

$$\overline{\mathbf{u}}_D = \phi \langle \overline{\mathbf{u}} \rangle^i, \quad \mathbf{u}_s = (1-\phi)\langle \mathbf{u} \rangle^s = const. \tag{11}$$

A relative velocity is then defined as,

$$\overline{\mathbf{u}}_{rel} = \overline{\mathbf{u}}_D - \mathbf{u}_s. \tag{12}$$

In addition, a relative Reynolds number based on $\overline{\mathbf{u}}_{rel}$ and D can be defined as:

$$\mathrm{Re}_D = \frac{\rho |\overline{\mathbf{u}}_{rel}| D}{\mu}. \tag{13}$$

Further, if one uses the Darcy velocity and the overall reactor size H, one has a different definition for Reynolds given by,

$$\mathrm{Re} = \frac{\rho |\overline{\mathbf{u}}_D| H}{\mu}. \tag{14}$$

Incorporating now in Eq. (2) a model for the Macroscopic Reynolds Stresses $-\rho\phi\langle \overline{\mathbf{u}'\mathbf{u}'} \rangle^i$, and assuming that a relative movement between

the two phases is described by Eq. (12), the momentum equation reads (see [6,7] for details),

$$\rho\left[\nabla \cdot \left(\frac{\overline{\mathbf{u}}_D \overline{\mathbf{u}}_D}{\phi} \right) \right] - \nabla \cdot \left\{ \left(\mu + \mu_{t_\phi} \right) \left[\nabla \overline{\mathbf{u}}_D + (\nabla \overline{\mathbf{u}}_D)^T \right] \right\} \tag{15}$$

$$= -\nabla\left(\phi \langle \overline{p} \rangle^i \right) - \frac{\mu\phi}{K} \overline{\mathbf{u}}_{rel} + \frac{c_F \phi \rho |\overline{\mathbf{u}}_{rel}| \overline{\mathbf{u}}_{rel}}{\sqrt{K}}$$

where μ_{t_ϕ} is the macroscopic eddy viscosity given by

$$\mu_{t_\phi} = \rho c_\mu f_\mu \frac{\langle k \rangle^{i^2}}{\langle \varepsilon \rangle^i}, \tag{16}$$

being c_μ a dimensionless constant and f_μ a damping function, which differs from unit if a Low-Reynolds turbulence model is applied. More on damping functions and model constants will be shown below. Thus, to obtain the eddy viscosity, μ_{t_ϕ}, we used here the Low and High Reynolds number k–ε models, whose equations for the turbulent kinetic energy and its dissipation rate, incorporating now a relative movement between the two phases $|\overline{\mathbf{u}}_{rel}|$, are given next [7].

A transport equation for $\langle k \rangle^i$ can be written as,

$$\rho\left[\nabla \cdot \left(\overline{\mathbf{u}}_D \langle k \rangle^i \right) \right] = \nabla \cdot \left[\left(\mu + \frac{\mu_{t_\phi}}{\sigma_k} \right) \nabla \left(\phi \langle k \rangle^i \right) \right] \tag{17}$$

$$-\rho\langle \overline{\mathbf{u}'\mathbf{u}'} \rangle^i : \nabla \overline{\mathbf{u}}_D + \underbrace{c_k \rho \frac{\phi \langle k \rangle^i |\overline{\mathbf{u}}_{rel}|}{\sqrt{K}}}_{G^i} - \rho\phi\langle \varepsilon \rangle^i$$

Table 1
Damping functions and constants for High and Low Reynolds turbulence models.

High Reynolds model proposed by Launder and Spalding [13]		Low Reynolds model proposed by Abe et al. [14]
f_μ	1.0	$\left\{1-\exp\left[-\frac{(\nu\varepsilon)^{0.25}y}{14\nu}\right]\right\}^2\left\{1+\frac{5}{(k^2/\nu\varepsilon)^{0.75}}\exp\left[-\left(\frac{(k^2/\nu\varepsilon)}{200}\right)^2\right]\right\}$
f_2	1.0	$\left\{1-\exp\left[-\frac{(\nu\varepsilon)^{0.25}y}{3.1\nu}\right]\right\}^2\left\{1-0.3\exp\left[-\left(\frac{(k^2/\nu\varepsilon)}{6.5}\right)^2\right]\right\}$
σ_k	1.0	1.4
σ_ε	1.33	1.3
c_1	1.44	1.5
c_2	1.92	1.9

where σ_k and c_k are dimensionless constants and the generation rate due to the porous substrate, G^i, which was included in Eq. (3), now depends on $|\overline{\mathbf{u}}_{rel}|$ and reads,

$$G^i = c_k \rho \phi \langle k\rangle^i |\overline{\mathbf{u}}_{rel}|/\sqrt{K}. \tag{18}$$

A corresponding transport equation for $\langle\varepsilon\rangle^i$, incorporating also the relative velocity $|\overline{\mathbf{u}}_{rel}|$, can be written as,

$$\rho\left[\frac{\partial}{\partial t}\left(\phi\langle\varepsilon\rangle^i\right) + \nabla\cdot\left(\overline{\mathbf{u}}_D\langle\varepsilon\rangle^i\right)\right] = \nabla\cdot\left[\left(\mu + \frac{\mu_{t_\phi}}{\sigma_\varepsilon}\right)\nabla\left(\phi\langle\varepsilon\rangle^i\right)\right]$$
$$+ c_1\left(-\rho\langle\overline{\mathbf{u}'\mathbf{u}'}\rangle^i : \nabla\overline{\mathbf{u}}_D\right)\frac{\langle\varepsilon\rangle^i}{\langle k\rangle^i} + c_2 c_k \rho\frac{\phi\langle\varepsilon\rangle^i|\overline{\mathbf{u}}_{rel}|}{\sqrt{K}} - c_2 f_2 \rho\phi\frac{\langle\varepsilon\rangle^{i^2}}{\langle k\rangle^i} \tag{19}$$

where σ_ε, c_1 and c_2 are constants and f_2 is a damping function.

2.3. Wall treatment and boundary conditions

In this work, two forms of the k–ε model are employed, namely the High Reynolds and Low Reynolds number turbulence models. For the High Reynolds turbulence model, a macroscopic form of the standard k–ε closure was used (Launder and Spalding [13]) whereas for the Low Reynolds number model constants and damping functions of Abe et al. [14] were applied. All model constants and damping functions for both turbulence models are compiled in Table 1.

Boundary conditions are given by:

On the solid walls (Low Reynolds turbulence model):

$$\overline{u} = 0, k = 0, \varepsilon = \nu\frac{\partial^2 k}{\partial y^2}. \tag{20}$$

On the solid walls (High Reynolds turbulence model):

$$\frac{\overline{u}}{u_\tau} = \frac{1}{\kappa}\ln\left(y^+ E\right), k = \frac{u_\tau^2}{c_\mu^{1/2}}, \varepsilon = \frac{c_\mu^{3/4}k_w^{3/2}}{\kappa y_w} \tag{21}$$

with, $u_\tau = \left(\frac{\tau_w}{\rho}\right)^{1/2}$, $y_w^+ = \frac{y_w u_\tau}{\nu}$, where u_τ is the wall-friction velocity, y_w is the non-dimensional coordinate normal to wall, κ is the von Kármán constant, and E is a constant that depends on the roughness of the wall. For smooth walls, $E = 9$.
On the entrance:

$$\overline{\mathbf{u}}_D = \mathbf{u}_{inlet} \tag{22}$$

At the exit, zero diffusion flux is considered for all variables.

Table 2
Cases and parameters used (High Reynolds turbulence model, Launder and Spalding [13]).

Cases investigated	Dimensional					Non-dimensional					
	u_D [m/s]	u_s [m/s]	u_{rel} [m/s]	D [m]	K [m²]	Re_D	Re	u_s/u_D	Da	ϕ	y+
Effect of Re_D	4.250E01	2.125E01	2.125E01	8.00E−03	1.000E−06	1.00E04	1.938E05	5.0E−01	1.665E−04	0.6	1.119E01
	2.120E02	1.062E02	1.062E02			5.00E04	1.938E06				4.762E01
	4.250E02	2.125E02	2.125E02			1.00E05	3.875E06				9.104E01
	4.250E03	2.125E03	2.125E03			1.00E06	3.875E07				8.267E02
Effect of u_s/u_D	4.250E02	0.000E00	4.250E02	8.00E−03	1.000E−06	2.00E05	3.875E06	0.0E00	1.665E−04	0.6	1.840E02
		1.062E02	3.188E02			1.50E02		2.5E−01			1.351E02
		2.125E02	2.125E02			1.00E05		5.0E−01			9.105E01
		3.187E02	1.063E02			5.00E04		7.5E−01			6.234E01
		4.037E02	2.125E01			1.00E04		9.5E−01			6.137E01
Effect of Da	4.250E02	2.125E02	2.125E02	1.00E−03	1.562E−08	1.25E04	3.875E06	5.0E−01	2.601E−06	0.6	1.170E02
				3.00E−03	1.406E−07	3.75E04			2.341E−05		1.081E02
				1.00E−02	1.562E−06	1.25E05			2.601E−04		8.690E01
Effect of ϕ	2.120E02	1.062E02	1.062E02	8.00E−03	1.975E−07	5.00E04	1.938E06	5.0E−01	3.289E−05	0.4	5.867E01
				3.50E−03	1.000E−06				1.665E−04	0.6	4.762E01
				1.30E−03	7.111E−06				1.184E−03	0.8	3.600E01

Table 3
Cases and parameters used (Low Reynolds turbulence model, Abe et al. [14]).

Cases investigated	Dimensional					Non-dimensional					
	u_D [m/s]	u_s [m/s]	u_{rel} [m/s]	D [m]	K [m²]	Re_D	Re	u_s/u_D	Da	ϕ	y+
Effect of Re_D	5.312E00	2.656E00	2.656E00	8.00E−03	1.000E−06	1.25E03	4.844E04	5.0E−01	1.665E−04	0.6	1.72E00
	1.062E01	5.312E00	5.312E00			2.50E03	9.688E04				2.88E00
	2.125E01	1.062E01	1.062E01			5.00E03	1.938E05				4.68E00
Effect of u_s/u_D	1.190E01	0.000E00	1.190E01	8.00E−03	1.000E−06	5.60E03	1.085E05	0.0E00	1.665E−04	0.6	1.86E00
		2.975E00	8.925E00			4.20E03		2.5E−01			1.80E00
		5.950E00	5.950E00			2.80E03		5.0E−01			1.72E00
		8.925E00	2.975E00			1.40E03		7.5E−01			1.58E00
Effect of Da	3.400E01	1.700E01	1.700E01	1.00E−03	1.562E−08	1.00E03	3.100E05	5.0E−01	2.601E−06	0.6	3.25E00
				3.00E−03	1.406E−07	3.00E03			2.341E−05		3.65E00
				1.00E−02	1.562E−06	1.00E04			2.601E−04		4.78E00
Effect of ϕ	1.062E01	5.312E00	5.312E00	8.00E−03	1.975E−07	2.50E03	9.688E04	5.0E−01	3.289E−05	0.4	3.19E00
				3.50E−03	1.000E−06				1.665E−04	0.6	3.18E00
				1.30E−03	7.111E−06				1.184E−03	0.8	3.20E00

3. Numerical method

The numerical method used to discretize the flow equations was based on the control volume approach. A schematic of node labeling for a general non-orthogonal two-dimensional grid is presented in Fig. 1b. The SIMPLE method of Patankar [15] was used to the handle the pressure–velocity coupling and applied to relax the systems of algebraic equations.

The discretized form of the two-dimensional conservation equation for a generic property φ in steady-state reads,

$$I_e + I_w + I_n + I_s = S_\varphi \tag{23}$$

where I_e, I_w, I_n and I_s represent, respectively, the fluxes of φ in the east, west, north and south faces of the control volume. S_φ represents the source term, whose standard linearization is accomplished by making,

$$S_\varphi \approx S_\varphi^{**} \langle \varphi \rangle_p^i + S_\varphi^*. \tag{24}$$

Discretization of the momentum equation in the x-direction gives further,

$$S^{*x} = \left(S_e^{*x}\right)_P - \left(S_w^{*x}\right)_P + \left(S_n^{*x}\right)_P - \left(S_s^{*x}\right)_P + S_P^* \tag{25}$$

$$S^{**x} = S_\phi^{**} \tag{26}$$

where, S^{*x} is the diffusive part, here treated in an explicit form. The second term, S^{**x}, entails the additional drag forces due to the porous matrix, which are here treated explicitly.

Convergence was monitored in terms of the normalized residue, which was set to be lower than 10^{-9}.

4. Results and discussion

As mentioned, the problem under investigation is turbulent flow through a channel completely filled with a moving layer of a porous material, as shown in Fig. 1a. Data for all runs for moving bed cases are detailed in Tables 2 and 3.
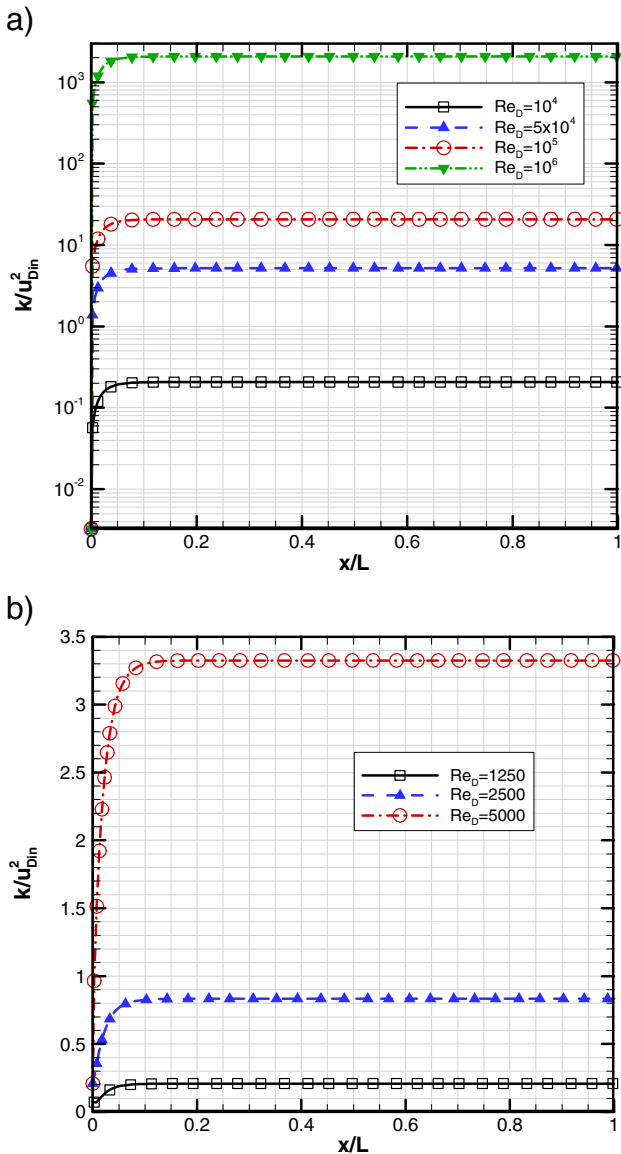
Fig. 2. Non-dimensional turbulent kinetic energy as a function of Re_D, with $u_s/u_D = 0.5$, $\phi = 0.6$: a) High Reynolds model and b) low Reynolds model.
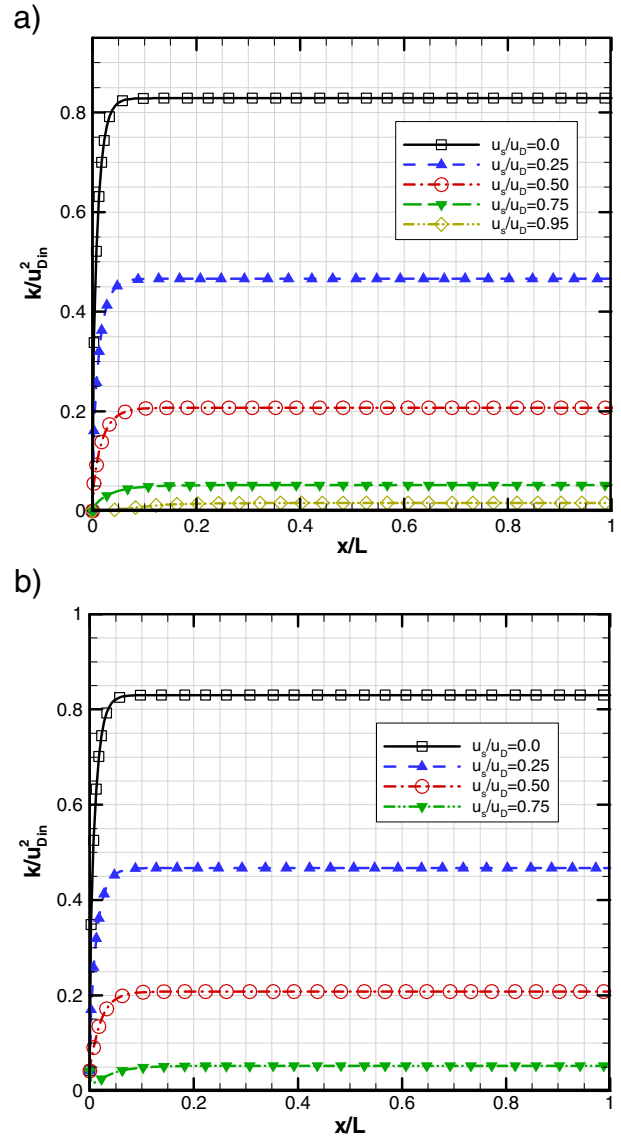
Fig. 3. Non-dimensional turbulent kinetic energy as a function of u_s/u_D, with $k_s/k_f = 25$, $\phi = 0.6$, $Da = 1.665 \times 10^{-4}$: a) High Reynolds model $Re_D \approx 10^5$, and b) Low Reynolds model $Re_D \approx 10^{13}$.

4.1. Effect of Reynolds number, Re_D

The Reynolds number Re_D was calculated based on relative velocity $\overline{\mathbf{u}}_{rel}$ for high and low Reynolds models. It is noticed that when Darcy velocity $\overline{\mathbf{u}}_D$ increases while keeping the same porosity and slip ratio, there is an increase in the relative velocity $\overline{\mathbf{u}}_{rel}$ (see Tables 2 and 3). Accordingly, Fig. 2a and b shows that when the relative velocity increases, a greater amount of mean mechanical energy is converted into turbulence, regardless of the turbulence model used. Or say, as the relative fluid velocity increases past the solid obstacles, the amount of fluid disturbance is increased leading to an increase in the final level of $\langle k \rangle^i$. That can be seen by inspecting the generation term $G^i = c_k \rho \phi \langle k \rangle^i |\overline{\mathbf{u}}_{rel}|/\sqrt{K}$ that is proportional to $\overline{\mathbf{u}}_{rel}$.

4.2. Effect of slip ratio, $\mathbf{u}_s/\overline{\mathbf{u}}_D$

Fig. 3a and b indicates the damping of turbulence as the solid velocity approaches that of the flowing fluid. As the relative velocity $\overline{\mathbf{u}}_{rel}$ decreases, the amount of disturbances in the flow is reduced, implying

then in a reduction of the final level of $\langle k \rangle^i$, according to G^i for both High and Low Reynolds number models.

4.3. Effect of Darcy number, Da

Fig. 4 shows the distribution of turbulence kinetic energy with variation of Darcy number. It is notice that as Darcy number increases, the intensity of the turbulence kinetic energy inside of the porous layer decreases, mainly next to the entrance, staying constant along the channel after $x/L = 0.15$ for High (Fig. 4a) and Low Reynolds (Fig. 4b) models.

4.4. Effect of porosity, ϕ

Fig. 5 shows the values for non-dimensional turbulent kinetic energy along the channel as a function of porosity ϕ and for both turbulence models here employed. The Reynolds number, Re_D, and the velocity ratio between the solid and fluid phases, $u_s/u_D = 0.5$, are kept constant for all curves in the figure.

a)

b)
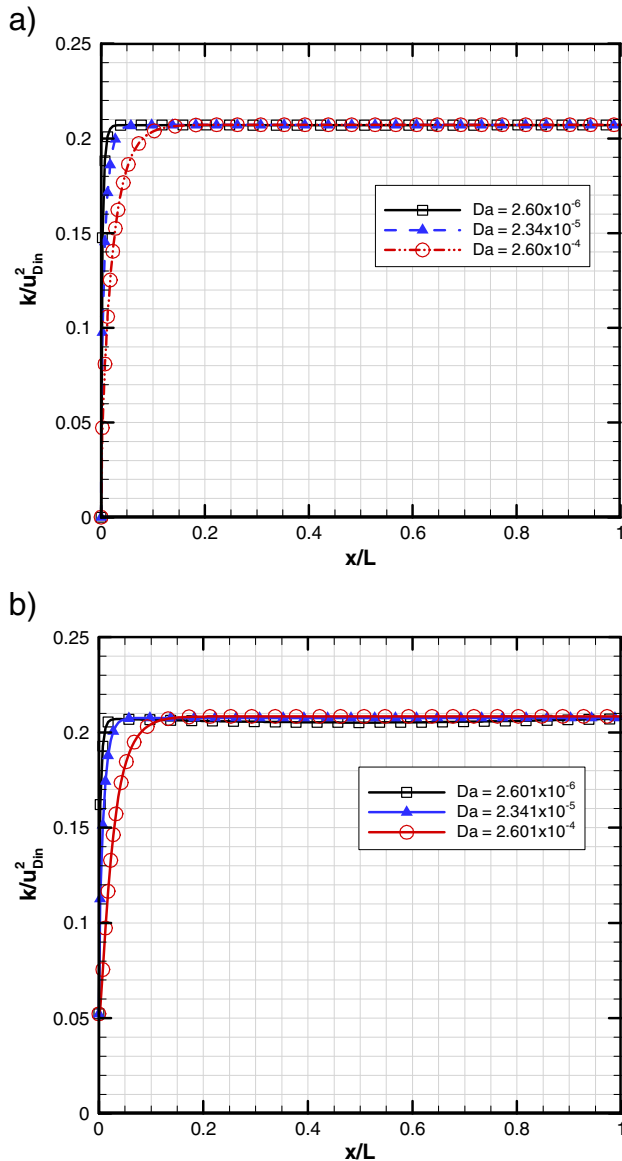
Fig. 4. Non-dimensional turbulent kinetic energy as a function of Da, with $u_s/u_D = 0.5$, $\phi = 0.6$: a) High Reynolds model, $Re = 3.875 \times 10^6$; and b) Low Reynolds model, $Re = 3.1 \times 10^5$.

a)

b)
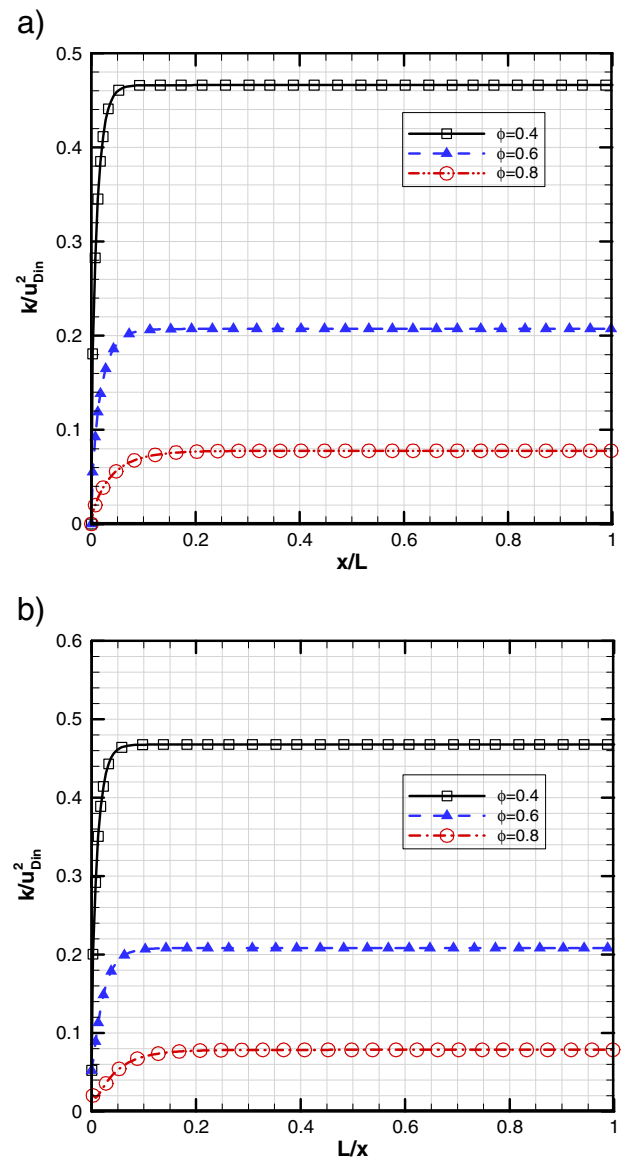
Fig. 5. Non-dimensional turbulent kinetic energy as a function of ϕ, with $u_s/u_D = 0.5$: a) High Reynolds model, $Re_D = 5 \times 10^4$; and b) Low Reynolds model $Re_D = 2.5 \times 10^3$.

For a fixed Reynolds number based on $\overline{\mathbf{u}}_D = \phi\langle\overline{\mathbf{u}}\rangle^i$, a decrease in porosity corresponds to an increase in the intrinsic fluid velocity $\langle\overline{\mathbf{u}}\rangle^i$, reflecting a greater conversion of mean mechanical kinetic energy into turbulence. It is also observed that as the porosity gets lower, while keeping both velocities constant, the permeability K decreases leading to an increase in the final level of $\langle k\rangle^i$ according to G^i (see Eq. (18)), which is, as seen, the generation rate of $\langle k\rangle^i$ due the porous substrate.

5. Conclusions

This paper investigated the behavior of turbulent kinetic energy in a concurrent moving porous bed. Numerical solutions for turbulent flow were obtained for different Reynolds number, Re_D, slip ratio, $\mathbf{u}_s/\mathbf{u}_D$, Darcy number, Da and porosity ϕ. Governing equations were discretized and numerically solved.

It is observed, according with the results obtained, that for high values of Re_D, higher final levels of $\langle k\rangle^i$ are simulated, as expected. The same effect occur for lower values of slip ratio $\mathbf{u}_s/\overline{\mathbf{u}}_D$, Darcy number Da and porosity ϕ, or say, for smaller values of these parameters, higher levels of $\langle k\rangle^i$ are computed. Results herein might be useful to the design and analysis of a number of engineering processes of practical interest.

Acknowledgments

References

[1] Y. Yang, M. Hwang, Numerical simulation of turbulent fluid flow and heat transfer characteristics in heat exchangers fitted with porous media, Int. J. Heat Mass Transf. 52 (2009) 2956–2965.

[2] H. Littman, M.H. Morgan III, S.D. Jovanovic, J.D. Paccione, Z.B. Grbavcic, D.V. Vukovic, Effect of particle diameter, particle density and loading ratio effective drag coefficient in steady turbulent gas–solids transport, Powder Technol. 84 (1995) 49–56.

[3] Z. Mansoori, M. Saffar-Avval, H. Basirat-Tabrizi, G. Ahmadi, S. Lain, Thermo-mechanical modeling of turbulent heat transfer in gas-solid flows including particle collisions, Int. J. Heat Fluid Flow 23 (2002) 792–806.

[4] Y. Zhang, J.M. Reese, Particle–gas turbulence interactions in a kinetic theory approach to granular flows, Int. J. Multiphase Flow 27 (2001) 1945–1964.

[5] M.J.S. de Lemos, C. Fischer, Thermal analysis of an impinging jet on a plate with and without a porous layer, Numer. Heat Transf. Part A Appl. 54 (2008) 1022–1041.

[6] M.J.S. de Lemos, Turbulence in Porous Media: Modeling and Applications, 2nd. ed. Elsevier, Amsterdam, 2012.

[7] M.J.S. de Lemos, M.B. Saito, Computation of turbulent heat transfer in a moving porous bed using a macroscopic two-energy equation model, Int. Commun. Heat Mass Transf. 35 (2008) 1262–1266.

[8] A.C. Pivem, M.J.S. de Lemos, Laminar heat transfer in a moving porous bed reactor simulated with a macroscopic two-energy equation model, Int. J. Heat Mass Transf. 55 (2012) 1922–1930.

[9] A.C. Pivem, M.J.S. de Lemos, Temperature distribution in a counterflow moving bed under a thermal nonequilibrium condition, Numer. Heat Transf. 61 (1–17) (2012).

[10] W.G. Gray, P.C.Y. Lee, On the theorems for local volume averaging of multiphase system, Int. J. Multiphase Flow 3 (1977) 333–340.

[11] S. Whitaker, Advances in theory of fluid motion in porous media, Ind. Eng. Chem. 61 (1969) 14–28.

[12] S. Whitaker, Diffusion and dispersion in porous media, J. Am. Inst. Chem. Eng. 13 (3) (1967) 420–427.

[13] B.E. Launder, D.B. Sapalding, The numerical computation of turbulent flows, Comput. Methods Appl. Mech. Eng. 3 (1974) 269–289.

[14] K. Abe, Y. Nagano, T. Kondoh, An improve k–ε model for prediction of turbulent flows with separation and reattachment, Trans. JSME 58 (1992) 3003–3010.

[15] S.V. Patankar, Numerical Heat Transfer and Fluid Flow, Hemisphere, Washington, DC, 1980.